ORIGINAL ARTICLE

Veterinary Research Forum. 2022; 13 (4) 501 - 506
doi: 10.30466/vrf.2021.527750.3161
Journal Homepage: vrf.iranjournals.ir

Veterinary Research Forum

In silico prediction of amino acids involved in cCPE$_{290-319}$ interaction with claudin 4

Yousef Sharafi, Seyed Ali Mirhosseini, Jafar Amani*

Applied Microbiology Research Center, Systems Biology and Poisonings Institute, Baqiyatallah University of Medical Sciences, Tehran, Iran.

Article Info

Article history:

Received: 07 April 2021
Accepted: 15 June 2021
Available online: 15 December 2022

Keywords:

Claudin
Clostridium perfringens
Interaction
Molecular dynamics simulation

Abstract

Among the 26 human claudin proteins, the food-poisoning bacterium *Clostridium perfringens* produces an enterotoxin (~ 35.00 kDa) that specifically targets human claudin 4, causing diarrhea by fluid accumulation in the intestinal cavity. The *Clostridium perfringens* enterotoxin (CPE) C-terminal domain (cCPE ~ 15.00 kDa) tightly binds to claudin 4 and disrupts the tight junction barriers in the intestines. In this study, we aimed to determine the contribution and type of amino acid interactions involved in association between claudin 4 and the C-terminal CPE. First, the three-dimensional format of claudin 4 was downloaded from RCSB. Then, during 60.00 nanoseconds (nsec), molecular dynamics simulation was conducted using the GROMACS package on CPE of crystallographic structure. The results indicated that the simulations performed well during the simulation times and there were no noticeable problems or artifacts. We found that Coulombic (glycine 317, proline 311 and serine 313) and Lennard-Jones (tyrosine 310, leucine 315, serine 313 and glycine 317) interactions played a significant role in complex stability. This information localized the C-terminal of CPE as a linear sequence sufficient for recognition and binding to the eukaryotic CPE receptor. A detailed description of the dissociation process brings valuable insight into the interaction of the claudin 4-cCPE$_{290-319}$ complexes, which could help in the future to design more potent drugs.

Introduction

Claudins are a family of 17.00 - 27.00 kDa integral membrane proteins that form the backbone of tight junctions between the epithelial cells and regulate epithelial and endothelial paracellular permeability.[1,2] The claudin family consists of 23 transmembrane proteins with distinct tissue and developmental expression, which can promote *Clostridium perfringens* enterotoxin (CPE) binding and cytolysis.[1,3] Such proteins may form homodimers or heterodimers to produce paired strands that connect adjacent cells and thus determine the characteristic properties of different epithelial tissues.[4] Researchers using gene expression profiling found that the genes claudin 3 and claudin 4 were highly expressed in ovarian, uterine, colorectal, breast, prostate and pancreatic cancers,[5-12] suggesting they might have a beneficial impact on tumorigenesis and could contribute to improved invasion, motility and cell survival.[7] In fact, claudin 4 is expressed in about 70.00 - 90.00% of different cancers and is found uniformly across subtypes with the lowest expression seen in the clear cell subtype.

The key role that claudin 4 plays in different types of cancers is still unclear and these tight junctions (TJ) proteins have recently been shown to be the naturally occurring *Clostridium perfringens* enterotoxin (CPE) receptors. CPE causes one of the most common food poisoning agents in the United States and Europe to have gastrointestinal symptoms.[13] Additionally, CPE is thought to contribute to diarrhea consistent with antibiotic therapy and too often induce gastrointestinal illness in domestic animals.[14,15] The CPE binds to claudin 3 and claudin 4, initially known as CPE-receptors and some other members of the claudin family, which are tight junction proteins.[16] CPE cytotoxicity is a multistep process that initiates an extracellular loop of CPE binding on specific members of the claudin family of tight junction proteins.[3] This is followed by the formation of ~ 450 and ~ 600 kDa SDS-resistant complexes which contain CPE and claudins. The ~600 kDa complex also contains a second tight transmembrane protein, occludin.[17,18] After CPE-binding to claudins via the C-terminal domain (cCPE), the formation of pores in the plasma membrane of the host mucosa cell results in fluid and electrolyte loss along with epithelial

***Correspondence:**

Jafar Amani. PhD
Applied Microbiology Research Center, Systems Biology and Poisonings Institute, Baqiyatallah University of Medical Sciences, Tehran, Iran
E-mail: jamani5@bmsu.ac.ir

cell death, known as CPE-intoxication clinical symptoms.[19]

Analysis of the CPE structure-function relationship by characterizing the functional properties of enterotoxin fragments revealed that the COOH-terminal 30 amino acid fragment of CPE ($cCPE_{290-319}$) does not cause cytolysis but maintains a high binding affinity to the claudins. This fragment also completely blocks the specific binding of the full-length toxin, thus, eliminating the cytolysis of susceptibility target cells.[20] While it remains potentially immunogenic, the domain $cCPE_{290-319}$ contains fewer antigenic determinants than the COOH-terminal half of the CPE molecule.[21] Removal of these residues prevents binding and a fusion protein comprising only these residues may compete to bind to isolated brush border membranes with full-length CPE.[20] The removal of the last five amino acids was sufficient in other studies to completely abrogate binding,[22] although it remains unclear whether these residues contain the binding site or whether their removal is destabilizing the protein. These results indicated that the fragment of the CPE peptide might be used to target CPE-based toxins to claudins on various cancer cells that express high claudin 4 levels.

Computer simulation techniques have been very valuable instruments for recognizing and investigating the physical foundations of bio-macromolecules structure and function. The application of computer simulation in structural and dynamic protein studies and the understanding of protein folding and unfolding mechanisms at atomic details have been the subject of much research for many years.[23,24] Simplified and all-atomic simulations of molecular dynamics (MD) are common computing methods in this area.[25,26] However, all-atomic MD simulations with explicit solvent are more preferred. They have high time and space resolution that enable a detailed comparison of the energetic and structural properties of a protein at different temperatures, and provide a large amount of information not directly accessible from the laboratory experiment.[27,28]

This study was performed to determine the contribution and type of amino acid interactions involved in association between claudin 4 and the cCPE.

Materials and Methods

Protein preparation. Crystallographic structure of claudin 4 and CPE complex was retrieved from the Structural Bioinformatics Protein Data Bank Research Collaboratory (http:/www.rcsb.org/pdb/home/home.do) and the structure with PDB ID 5B2 G,[29] was used in the present study.

Molecular dynamics simulation. Simulation of molecular dynamics was carried out using the Gromacs vesion 5.1.2 package (University of Groningen, Groningen, Netherlands).[30] Systems were solvated in a cubic box with simple point charge (SPC) water molecules at 1.00 nm marginal radius. The structures were observed to be negatively charged at physiological pH, thus, to make the simulation system electrically neutral, we added 10.00 sodium ions (Na^+) to the simulation box using the "gmx genion" tool accompanying the gromac package. After this, the whole molecular system was subjected to energy minimization by the steepest descent algorithm. Briefly, after energy minimization, the whole molecular system was equilibrated with the protein fixed in the NVT ensemble for 100 picosecond (psec) using a 2.00 femtosecond (fsec) time step and a target temperature of 310 K. Further 1,000 psec equilibration was applied in the NPT ensemble at 310 K using a 2.00 fsec time step. The Berendsen temperature coupling method[31] was used to control the temperature inside the box. Electrostatic interactions have been measured using the Particle Mesh Ewald method.[32] The pressure was held at 1.00 atm with an acceptable compressibility scale of 4.50×10^{-5} atm. SHAKE algorithm was used to constrain bond lengths containing hydrogen, requiring a time stage of 2.00 fsec. Van der Waals and Coulomb interactions were truncated to 1.00 nm. The non-bonded pair list has been updated every 10 steps and the conformations have been stored every 2.00 psec. In the end, the systems were subjected to 60.00 nanosec MD simulation in NPT ensemble (310 K, 1.00 atm). The root-mean-squared deviation (RMSD) and root-mean-square fluctuation (RMSF) analyzes were conducted using gmx rms and gmx RMSF modules in Gromacs, respectively. Further analysis was conducted with the Gromacs package and UCSF chimera software version 1.16 (The Resource for Biocomputing, Visualization, and Informatics (RBVI) at the University of California, San Francisco, USA).[33]

Results

The most stable position for connection of CPE to claudin 4 is seen in Figure 1. In this Figure, the CPE (red and violet) is located at the best binding site at the lowest energy level of the claudin 4 (Figs. 1A and 1B).

The structure of cCPE in the claudin 4 complex was almost the same as that of the CPE protein itself, suggesting the absence of a conformational modification of the cCPE in complex formation. The two extracellular parts, ECS1 and ECS2 of claudin 4, both interacted with cCPE and the complex represented the left hand of the ellipsoidal cCPE (Fig. 1C).

The results of the RMSD study showed that no instability was observed during the simulation time for the cCPE-claudin 4 complex (Fig. 2A). For the cCPE-claudin 4 complex, the RMSD value was less than 4.60 Å. This suggested that the initial cCPE-claudin 4 contacted stayed intact throughout the simulation process. The slope of the RMSD graph indicated that the model was stable

throughout simulation time (10.00 nsec). The closer the slope was to zero, the more stable the model was simulated, and the more gradually the slope increased or fluctuated, the more unstable the model would become.

Another diagram that shows the correct method of the simulation process is the energy diagram (Fig. 2B). Unlike the RMSD chart, a decrease in the energy chart slope indicated better simulation quality because less energy was obtained in a more stable state. The energy changes in this graph after the beginning of the process decrease in the rest of the path were accompanied by a constant fluctuation and therefore the model made over time was a stable simulation. However, in the energy diagram of this simulation, the molecular dynamics of the oscillation interval were much less than this value.

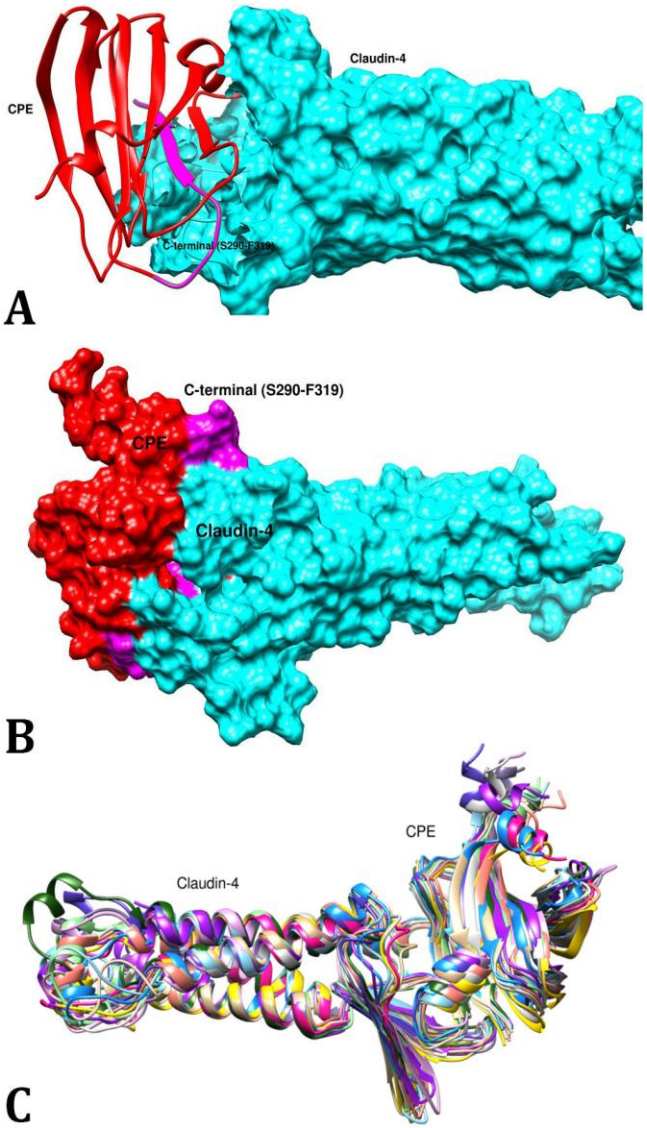

Fig 1. Three-dimensional diagram of the interaction of cCPE$_{290-319}$ with claudin 4. **A** and **B)** The CPE position within claudin 4, **C)** Position of two extracellular parts, ECS1 and ECS2 of claudin 4.

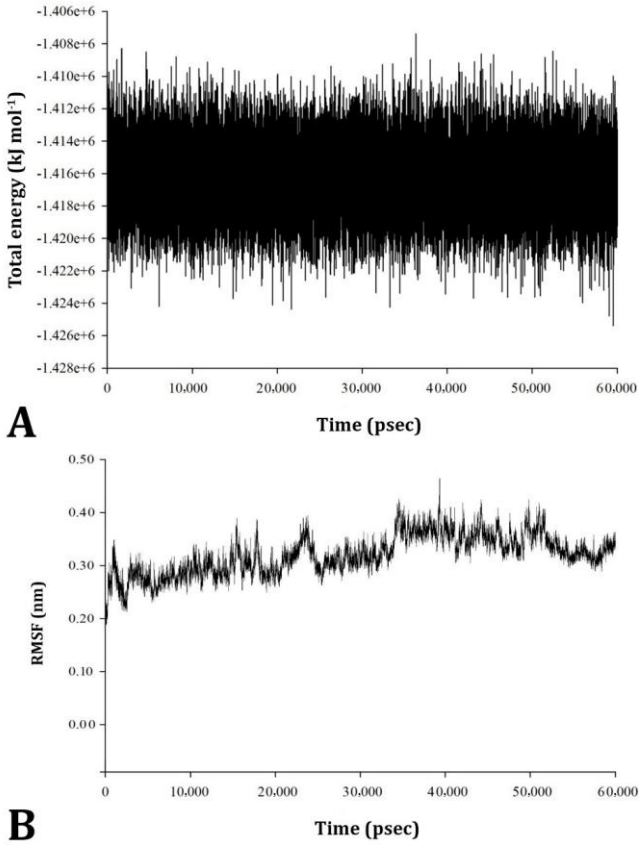

Fig. 2. The total energy and root mean square deviations (RMSD) as functions of the claudin-cCPE$_{290-319}$ molecular dynamic (MD) simulation time. **A)** The total energy of the whole claudin-cCPE$_{290-319}$ structure; **B)** The backbone RMSD of cCPE structure.

The RMSD is not a suitable parameter for reflecting the mobility of structural elements and the RMSF was used to examine the flexibility of the structure. The RMSF of the trajectory from the MD simulation for the claudin 4-cCPE$_{290-319}$ complex was calculated, and the protein residual fluctuations in claudin 4-cCPE$_{290-319}$ complexes were minimal (Fig. 3). The RMSF plot revealed very mild fluctuations in amino acids indicating the uninterrupted interaction between CPE and claudin 4, while a small region (266 - 270 CPE residues) in the plot showed the highly flexible regions in the complex (Fig. 3).

Higher peaks in the small CPE regions have shown that it undergoes high fluctuations through significant conformational changes. Overall, the RMSF values lying within the 0.10 - 0.25 nm range indicated the claudin 4 stable binding. Claudin 4 with mild fluctuations formed the various arrangements in the proximity of the protein CPE binding site. A similar conclusion could be drawn from the contact map obtained for the simulation studies.

Claudin 4's interaction energy with cCPE$_{290-319}$ protein residues within 4.00 Å was calculated over the entire MD trajectory. The energy of residue interaction for 60.00 nsec is shown in Table 1.

Two types of short-range potentials were calculated: Lennard-Jones short-range (LJ-SR) and Coulombic short-range (Coul-SR) potential. The sum of LJ-SR and Coul-SR potential obtained was consistent with claudin 4-cCPE$_{290-319}$ complex experimental activity.

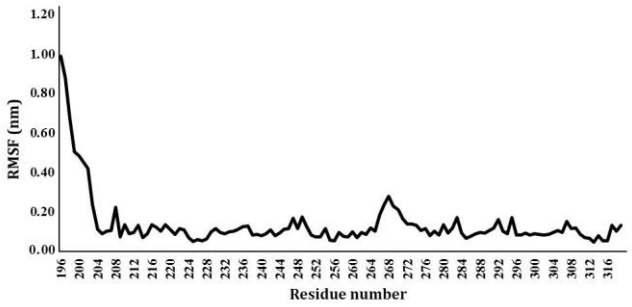

Fig. 3. Residue RMSF of the claudin 4-cCPE$_{290-319}$ complexes from the generated model during the trajectory period of 60.00 nsec MD simulation.

Table 1. The Coulombic short-range (Coul-SR) and Lennard-Jones short-range (LJ-SR) interaction between claudin 4 and residues of cCPE$_{290-319}$ in the neighborhood.

Residue number	Coul-SR (kJ mol^{-1})	LJSR (kJ mol^{-1})	Sum
Serine 290	-1.29	- 6.05	- 4.76
Leucine 291	+1.98	- 2.46	- 0.48
Aspartic acid 292	0.00	0.00	0.00
Alanine 293	0.00	0.00	0.00
Glucine 294	0.00	0.00	0.00
Glutamine 295	+3.31	- 2.05	1.26
Tyrosine 296	0.00	0.00	0.00
Valine 297	0.00	0.00	0.00
Leucine 298	0.00	0.00	0.00
Valine 299	0.00	0.00	0.00
Methionine 300	+ 0.02	- 0.43	- 0.41
Lysine 301	+ 0.06	- 0.42	- 0.37
Alanine 302	+ 0.52	- 2.74	- 2.22
Asparagine 303	+ 0.03	- 0.25	- 0.23
Serine 304	- 0.07	- 0.33	- 0.40
Serine 305	- 0.03	- 0.20	- 0.22
Tyrosine 306	- 0.70	- 12.03	- 12.73
Serine 307	- 0.07	- 0.34	- 0.41
Glycine 308	- 0.04	- 0.33	- 0.37
Asparagine 309	- 0.22	- 1.24	- 1.46
Tyrosine 310	- 0.27	- 37.78	- 38.05
Proline 311	- 16.64	- 11.65	- 28.29
Tyrosine 312	- 0.46	- 11.64	- 12.11
Serine 313	- 8.82	- 16.27	- 25.10
Isoleucine 314	- 3.57	- 5.31	- 8.88
Leucine 315	+ 0.48	- 20.14	- 19.66
Phenylalanine 316	+ 0.08	- 0.87	- 0.79
Glycine 317	- 25.49	- 15.05	- 40.53
Aspartic acid 318	- 0.63	- 1.81	- 2.43
Phenylalanine 319	- 0.37	- 7.47	- 7.84
Sum	- 52.14	-156.87	- 209.05

The results showed that the amount of energy interacting Coul-SR and LJ-SR for cCPE$_{290-319}$ was - 52.53 and - 156.87 kJ mol^{-1}, respectively. The results showed that amino acids of glycine 317, proline 311 and serine 313 had the highest amount of Coul-SR interaction energy. Also, the amino acids of tyrosine 310, leucine 315, serine 313 and glycine 317 have the highest LJ-SR interaction energy. In general, the amino acids glycine 317, tyrosine 310, proline 311, serine 313, leucine 315, tyrosine 306, tyrosine 312, isoleucine 314 and phenylalanine 319 had the highest Coul-SR and LJ-SR interaction energy.

Discussion

The findings of this study provided an integral part of our compounds' pre-clinical investigation that could be further developed as tumor anticancer agents, with excellent oral absorption. In this study, we aimed to determine the contribution and type of amino acid interactions involved in the association between claudin 4 and the C-terminal CPE. The aim was to analyze numerous parameters responsible for the stabilization of cCPE-claudin 4 complexes and to recognize the key residues in the cCPE-claudin 4 binding which could be further exploited for the design and production of potent drugs. We first performed an MD simulation analysis to implement our theory and then binding free energy of the CPE-claudin 4 complexes. At present, techniques such as MD simulation, metadynamics, and the US are widely used to address many atomistic biological phenomena. Therefore, as we decided to take crystal structures directly for the study of MD simulation, 60.00 nsec simulation was performed to balance the system. In our study, we investigated in-depth, using several analytical techniques to understand the fundamental mechanism behind this complex interaction mechanism of CPE-claudin 4. From the simulation results, it is clear that CPE-claudin 4 complexes showed an RMSD of less than 4.60 Å. The RMSD and RMSF plots enabled the assessment of cCPE's dynamic behavior in complex claudin 4 and amino acid residue fluctuations upon cCPE binding. Moreover, these analyses showed that cCPE$_{290-319}$ reached conformational stability after interaction with the claudin 4. Nonetheless, for this receptor type, the RMSD and RMSF plots displayed the most important conformational changes and the greatest number of hydrogen bonds affected main amino acid residues. The complete flexibility analysis resulted in the cCPE's stable binding with claudin 4 receptor suggested the cCPE's high potency against the target claudin 4 receptor. Hence, RMSD plot are important to transfer out the prediction of structural stability on protein.[34,35]

From the MD simulations, we decided to determine the individual contribution of residues to the energy of the interaction. Potential energies for LJ-SR and Coul-SR were determined. The sum of this surrounding 4.00 Å residue LJ-SR and Coul-SR potential for the individual cCPE$_{290-319}$ was consistent with the activity. After 60 nsec, cCPE$_{290-319}$ showed the value of – 209.53 kJ mol^{-1} potential. Glycine

317 showed the highest potential for Coul-SR with claudin 4, reflecting its utmost importance for the strong electrostatic interaction which might be responsible for the highest potency of claudin 4. The amount of potential for LJ-SR and Coul-SR could contribute to the estimation of energy interaction with other residues, such as tyrosine 310, proline 311, serine 313, leucine 315, tyrosine 306, tyrosine 312, isoleucine 314 and phenylalanine 319 which would account in both stability and potency. The results of this study confirmed the results of other studies.[15,20-22,29,36-38]

It has been shown that the site within cCPE responsible for the interaction with claudin 4 is confined to the fragment consisting of C-terminal residues 290 - 319 ($cCPE_{290–319}$), both based on radioligand binding experiments using 125I-labeled cCPE fragments[20] and based on surface plasmon resonance.[13] Tumor-targeting capacity of the 30-mer peptide *in vivo* has been reported in a mouse xenograft model of ovarian cancer for fluorescein-conjugated $cCPE_{290–319}$.[37] Residues of cCPE that are critical for its interaction with Claudin 4 were identified by an alanine scan of the protein's 16 C-terminal amino acids.[37] This and other experiments have shown that tyrosine 306, 310 and 312 and leucine 315 are critical for receptor binding,[38] which are located in a flexible loop between β sheets 8 and 9, i.e. residues lysine 304–tyrosine 312, or β sheet 9, depending on the crystal structure, respectively. Rather recently, the analysis of the X-ray crystal structure of cCPE complexed with lipid bilayer-embedded claudin 4 has restricted these findings.[29]

In general, a combined approach of MD simulation, energy interaction calculations and binding free energy estimates is useful for drug design and development. Using multiple analytical techniques and different approaches to drug design (virtual screening, fragment-based design, and de novo design), researchers could reduce failure and speed up the drug design process. These results indicated that the simulations were performing well during simulation times and no noticeable problems or artifacts were present. The results of this study, conducted in an environment of simulation and molecular dynamics, showed that CPE bound well at the lowest energy level to the claudin 4 structure. In the current study, we determined the structure of CPE's COOH-terminal domain, residues 290 - 319, which approximated the domain cCPE used by others for functional studies, and included the claudin-binding site. The residues of glycine 317, tyrosine 310, proline 311, serine 313, leucine 315, tyrosine 306, tyrosine 312, isoleucine 314 and phenylalanine 319 would be essential for their interaction, which was bound to claudin 4 since they developed hydrophobic contacts with claudin 4. In addition, CPE's subtype-specific, high-affinity interaction with claudins suggested the use of non-toxic or toxic CPE-based claudin modulators to improve drug delivery, diagnosis of carcinoma or carcinoma treatment. However, a more detailed study of structure-function is needed to (i) fully understand CPE-mediated pore formation and cellular downstream events and (ii) to develop effective peptide CPE-based biological activity for clinical use. In summary, the availability of a $cCPE_{290–319}$ structure suggested an unsuspected shared origin for the receptor-binding domains of multiple bacterial toxins and should allow rational protein modifications for future therapeutic applications.

Acknowledgments

The authors appreciate the excellent technical assistance of Mr. Kaveh Haji-Allahverdipour of the Department of Agricultural Biotechnology, Tarbiat Modares University, Tehran, Iran.

Conflict of interest

The authors have no conflict of interest to declare.

References

1. Tsukita S, Furuse M, Itoh M. Multifunctional strands in tight junctions. Nat Rev Mol Cell Biol 2001; 2(4): 285-293.
2. Krause G, Winkler L, Mueller SL, et al. Structure and function of claudins. Biochim Biophys Acta 2008; 1778(3): 631-645.
3. Katahira J, Sugiyama H, Inoue N, et al. Clostridium perfringens enterotoxin utilizes two structurally related membrane proteins as functional receptors in vivo. J Biol Chem 1997; 272(42): 26652-26658.
4. Sasaki H, Matsui C, Furuse K, et al. Dynamic behavior of paired claudin strands within apposing plasma membranes. Proc Natl Acad Sci U S A 2003; 100(7): 3971-3976.
5. Lu KH, Patterson AP, Wang L, et al. Selection of potential markers for epithelial ovarian cancer with gene expression arrays and recursive descent partition analysis. Clin Cancer Res 2004; 10(10): 3291-3300.
6. Nichols LS, Ashfaq R, Iacobuzio-Donahue CA. Claudin 4 protein expression in primary and metastatic pancreatic cancer: support for use as a therapeutic target. Am J Clin Pathol 2004; 121(2): 226-230.
7. Morin PJ. Claudin proteins in human cancer: promising new targets for diagnosis and therapy. Cancer Res 2005; 65(21): 9603-9606.
8. Santin AD, Zhan F, Cane' S, et al. Gene expression fingerprint of uterine serous papillary carcinoma: identification of novel molecular markers for uterine serous cancer diagnosis and therapy. Br J Cancer 2005; 92(8): 1561-1573.
9. Cheng TC, Manorek G, Samimi G, et al. Identification of genes whose expression is associated with cisplatin resistance in human ovarian carcinoma cells. Cancer Chemother Pharmacol 2006; 58(3): 384-395.

10. Kominsky SL, Tyler B, Sosnowski J, et al. *Clostridium perfringens* enterotoxin as a novel-targeted therapeutic for brain metastasis. Cancer Res 2007; 67(17): 7977-7982.
11. de Souza WF, Fortunato-Miranda N, Robbs BK, et al. Claudin-3 overexpression increases the malignant potential of colorectal cancer cells: roles of ERK1/2 and PI3K-Akt as modulators of EGFR signaling. PLoS One 2013; 8(9): e74994.doi:10.1371/journal.pone.0074994.
12. Kolokytha P, Yiannou P, Keramopoulos D, et al. Claudin-3 and claudin-4: distinct prognostic significance in triple-negative and luminal breast cancer. Appl Immunohistochem Mol Morphol 2014; 22(2): 125-131.
13. Ling J, Liao H, Clark R, et al. Structural constraints for the binding of short peptides to claudin-4 revealed by surface plasmon resonance. J Biol Chem 2008; 283(45): 30585-30595.
14. McClane BA. The complex interactions between *Clostridium perfringens* enterotoxin and epithelial tight junctions. Toxicon 2001; 39(11): 1781-1791.
15. Smedley JG 3rd, McClane BA. Fine mapping of the N-terminal cytotoxicity region of *Clostridium perfringens* enterotoxin by site-directed mutagenesis. Infect Immun 2004; 72(12): 6914-6923.
16. Fernández Miyakawa ME, Pistone Creydt V, Uzal FA, et al. *Clostridium perfringens* enterotoxin damages the human intestine in vitro. Infect Immun 2005; 73(12): 8407-8410.
17. Singh U, Van Itallie CM, Mitic LL, et al. Caco-2 cells treated with *Clostridium perfringens* enterotoxin form multiple large complex species, one of which contains the tight junction protein occludin. J Biol Chem 2000; 275(24): 18407-18417.
18. Singh AK, Jiang Y, Gupta S. Effects of bacterial toxins on endothelial tight junction *in vitro*: a mechanism-based investigation. Toxicol Mech Methods 2007; 17(6): 331-347.
19. Smedley JG 3rd, Uzal FA, McClane BA. Identification of a prepore large-complex stage in the mechanism of action of *Clostridium perfringens* enterotoxin. Infect Immun 2007; 75(5): 2381-2390.
20. Hanna P, Mietzner TA, Schoolnik GK, et al. Localization of the receptor-binding region of *Clostridium perfringens* enterotoxin utilizing cloned toxin fragments and synthetic peptides. The 30 C-terminal amino acids define a functional binding region. J Biol Chem 1991; 266(17): 11037-11043.
21. Sugii S. Analysis of multiple antigenic determinants of *Clostridium perfringens* enterotoxin as revealed by use of different synthetic peptides. J Vet Med Sci 1994; 56(6): 1047-1050.
22. Kokai-Kun JF, McClane BA. Determination of functional regions of *Clostridium perfringens* enterotoxin through deletion analysis. Clin Infect Dis 1997: Suppl 2: S165-S167.
23. Piseri P, Barborini E, Marino M, et al. Hydrogen uptake in cluster-assembled carbon thin films: experiment and computer simulation. J Phys Chem B 2004; 108(17): 5157-5160.
24. Daggett V. Protein folding– simulation. Chem Rev 2006; 106(5): 1898-1916.
25. Adcock SA, McCammon JA. Molecular dynamics: survey of methods for simulating the activity of proteins. Chem Rev 2006; 106 (5): 1589-1615.
26. van Gunsteren WF, Bakowies D, Baron R, et al. Biomolecular modeling: goals, problems, perspectives. Angew Chem Int Ed Engl 2006; 45(25): 4064-4092.
27. van Gunsteren WF, Mark AE. On the interpretation of biochemical data by molecular dynamics computer simulation. Eur J Biochem 1992; 204(3): 947-961.
28. van Gunsteren WF, Dolenc J, Mark AE. Molecular simulation as an aid to experimentalists. Curr Opin Struct Biol 2008; 18(2): 149-153.
29. Shinoda T, Shinya N, Ito K, et al. Structural basis for disruption of claudin assembly in tight junctions by an enterotoxin. Sci Rep 2016; 6: 33632. doi: 10.1038/ srep33632.
30. Hess B, Kutzner C, van der Spoel D, et al. GROMACS 4: algorithms for highly efficient, load-balanced, and scalable molecular simulation. J Chem Theory Comput 2008; 4(3): 435-447.
31. Berendsen HJC, van Postma JPM, van Gunsteren WF, et al. Molecular-dynamics with coupling to an external bath. J Chem Phys 1984; 81(8): 3684-3690.
32. Cheatham TE, Miller JL, Fox T, et al. Molecular dynamics simulations on solvated biomolecular systems: the particle mesh Ewald method leads to stable trajectories of DNA, RNA, and proteins. J Am Chem Soc 1995; 117(14): 4193-4194.
33. Sanner MF, Olson AJ, Spehner JC. Reduced surface: an efficient way to compute molecular surfaces. Biopolymers 1996; 38(3): 305-320.
34. Hospital A, Goñi JR, Orozco M, et al. Molecular dynamics simulations: advances and applications. Adv Appl Bioinform Chem 2015; 8: 37-47.
35. Kufareva I, Abagyan R. Methods of protein structure comparison. Methods Mol Biol 2012; 857: 231-257.
36. Takahashi A, Komiya E, Kakutani H, et al. Domain mapping of a claudin-4 modulator, the C-terminal region of C-terminal fragment of Clostridium perfringens enterotoxin, by site-directed mutagenesis. Biochem Pharmacol 2008; 75(8): 1639-1648.
37. Cocco E, Casagrande F, Bellone S, et al. Clostridium perfringens enterotoxin carboxy-terminal fragment is a novel tumor-homing peptide for human ovarian cancer. BMC Cancer. 2010; 10: 349. doi: 10.1186/ 1471-2407-10-349.
38. Veshnyakova A, Protze J, Rossa J, et al. On the interaction of *Clostridium perfringens* enterotoxin with claudins. Toxins (Basel) 2010; 2(6): 1336-1356.